Efficient Fabrication of Carbon Nanotube Point Electron Sources by Dielectrophoresis**

By *Jian Zhang*, *Jie Tang*, *Guang Yang*, *Qi Qiu*, *Lu-Chang Qin*, and *Otto Zhou**

Carbon nanotubes (CNTs) are being actively investigated as field-emission electron sources for a variety of electronic devices including displays,[1,2] X-ray tubes,[3] and electron microscopes.[4] Compared to the conventional field-emitters they have significantly improved emission characteristics, such as lower threshold field for emission,[5,6] higher emission current,[7,8] and improved stability.[9] In situ scanning electron microscopy (SEM) experiments have shown a stable emission current of 0.1–1 μA from an individual single-walled carbon nanotube (SWNT). A recent report demonstrates that field-emitted electrons from CNTs have a narrower spatial distribution and thus higher brightness compared to the state-of-art LaB$_6$ and Schottky electron sources,[4] which is desirable for precision vacuum electron devices. Efficient and reliable methods for fabrication of CNT point-emitters are, however, currently lacking. Direct growth of CNTs at predetermined locations has been demonstrated using chemical vapor deposition (CVD) techniques.[10–12] The approach requires selective deposition of nano- to micrometer-size catalysts and a high reaction temperature. In general it lacks control of the length, orientation, and number of CNTs grown. For laboratory experiments the CNTs can be manually attached to a sample holder coated with adhesives by a trial-and-error process.[13–16]

Dielectrophoresis is a powerful technique that can manipulate and assemble small objects into predetermined patterns by the interaction between the external electrical field and the induced dipole moments.[17] It has been applied to different systems.[18,19] Recently, we showed that CNTs can be assembled into submicrometer-diameter fibrils with controlled and variable lengths via the dielectrophoresis method.[20] In this paper, we report the fabrication of short CNT tips by this dielectrophoresis process, and their electron-field-emission properties. Aligned CNT tips comprising either SWNT bundles or multiwalled nanotubes (MWNTs) were assembled with controlled length and orientation. For the purpose of extracting stable emission current, the CNT tips were confined to 4–10 μm in length and 50–100 nm in diameter, with one end anchored on a tungsten wire. This method affords reliable control of the orientation, with all of the tips confined within a 2° angle from the cone axis of the W wire. A stable emission current of 3–5 μA was extracted.

SWNT bundles, produced by the laser-ablation method at the University of North Carolina (UNC), were first purified and etched to either ~0.5 μm or ~2 μm in bundle length by an oxidation process.[21] Prior experiments have shown that the processed materials maintain the basic characteristics of the nanotubes and are hydrophilic due to the presence of the COOH functional groups.[22–24] MWNTs produced by the plasma CVD method[25] were used without further processing. The nanotubes were dispersed in de-ionized water with the aid of sonication. The experimental setup comprises two electrodes, a chemically etched tungsten wire, and a metal holder, mounted on separate translation stages under an optical microscope. An alternating current (AC) field of 10 V at 2 MHz was applied between the W wire and the metal holder, which contained the nanotube/water suspension. Computer simulations using commercial software (Fig. 1) and experimental results have shown that the polarizable CNTs were attracted to the W tip where the electrical field gradient is high when the permittivity of the medium is lower than that of the nanotubes. To draw a continuous tip, the W electrode was translated horizontally to contact the surface of the suspension and was gradually withdrawn under the electrical field until a nanotube tip with a desired length was formed on the apex of the W wire.
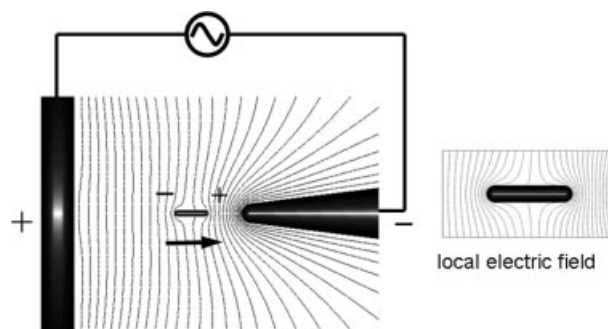
[*] Dr. O. Zhou, J. Zhang, Dr. J. Tang, G. Yang, Dr. L.-C. Qin
Department of Physics and Astronomy
University of North Carolina
Chapel Hill, NC 27599 (USA)
E-mail: zhou@physics.unc.edu
Dr. O. Zhou, C. Qin
Curriculum in Applied and Materials Sciences
University of North Carolina
Chapel Hill, NC 27599 (USA)
Q. Qiu
Xintek, Inc.
308 West Rosemary Street
Chapel Hill, NC 27516 (USA)
Dr. J. Tang
National Institute for Material Science
Tsukuba, 3050047 (Japan)

Figure 1. A schematic illustration of the dielectrophoresis assembly process. The electrical field distribution shown was simulated by a commercial package (LorentzE V6.0). The polarized CNTs in water were first aligned along the field direction due to the torque acting upon the induced dipole. When the permittivity of the object is larger than that of the medium the result shows a positive dielectrophoresis force driving the nanotubes towards the high field region, which is consistent with the theory [17]. The first group of CNTs adhered to the apex of the W tip and became the new outermost surface of the electrode where the next CNT precipitated. By gradual withdrawal of the W electrode from the liquid a continuous fibril was formed.

© 2004 WILEY-VCH Verlag GmbH & Co. KGaA, Weinheim　　1219

Ten samples were fabricated under similar conditions for this study. The length of the CNT tip was controlled by the travel distance of the W tip under the AC field. Figure 2a shows the scanning electron microscopy (SEM) image of one example. The individual nanotubes and the tip are aligned
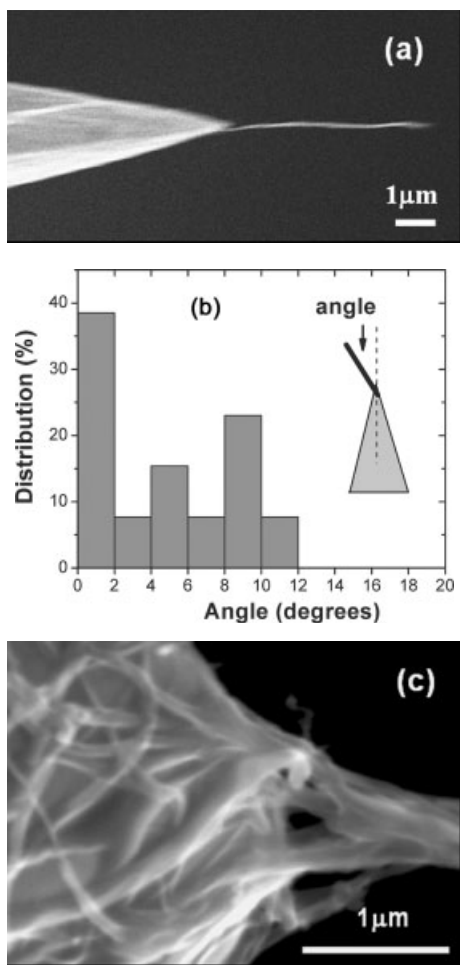

Figure 2. SEM image of a SWNT tip fabricated by the dielectrophoresis process with one end anchored on the apex of the W wire (a). A histogram obtained from measuring the angles between the CNT tips and the W wires (b). All the tips are confined within a 12° cone angle. At the CNT/metal interface entangled nanotubes adhered on the surface of the W wire and coagulated into a thin fibril with only a few nanotubes in the radial direction (c).

along the electrical field direction which is along the cone axis of the W. Figure 2b is the histogram obtained from measuring the angle formed by the CNT tip and the W wire. All the tips are confined within a 12° cone angle. The very end of the fibril comprises only a single SWNT bundle or a MWNT. At the CNT/metal interface entangled nanotubes adhere on the surface of the W wire and coagulate into a thin fibril with only a few nanotubes in the radial direction, as shown in Figure 2c for a MWNT tip.

The electron-field-emission characteristics of these tips were measured using point-plane geometry with a CNT tip mounted on a micrometer head as the cathode and an opposing metal plate as the anode. The distance between the two was adjusted by translating the micrometer head and was fixed to ~200 µm (estimated from the image taken using a charge coupled device (CCD) camera). The setup was then placed inside a vacuum chamber at 5×10^{-7} torr base pressure. The total emission current from the CNT tip was collected as a function of the applied voltage. Figures 3a,b show the data collected from a SWNT tip with a ~50 nm tip diameter. The emission current–voltage characteristics exhibited the classic Fowler–Nordheim type behavior with a linear relationship between $\ln(I/V^2)$ and $1/V$. The emission current reached 5 µA at less than 1000 V applied voltage, giving an estimated current density of 2.5×10^5 A cm^{-2}.

The emission stability was measured by monitoring the variation of the emission current with time for 10 h continuously in direct current (DC) mode at a fixed voltage. Figure 3c shows the data from a SWNT tip (~50 nm in diameter) measured sequentially at three different voltages. The emission current was stable at 1 µA and 2.8 µA when the applied voltage was fixed at 800 V and 1000 V, respectively, with no overall decay of the emission current. With a ballast resistor in series with the cathode, the local current fluctuation was calculated to be 5 % at 1 µA and 2.5 % at 2.8 µA. The emission current from the same sample reached 5.5 µA when the voltage was further increased to 1200 V, but suddenly dropped to zero after 1 h. No current was detected even at a higher voltage. SEM examinations revealed catastrophic failure from fracture of the W wire, and disappearance of the entire CNT tip as shown in Figure 3c inset. It is attributed to resistive heating at the W and CNT interface. In another SWNT tip, a stable current of 6.5 µA was obtained. The current fluctuation of this sample without the ballast resistor was about 12 %, comparable to value reported from a un-ballasted individual SWNT.[26]

In some samples, segmentation of the CNT tips occurred first, typically when the current was raised to above 5 µA, which resulted in a sudden decrease of the emission current. The current could be recovered by increasing the applied voltage. This process repeated several times until no current could be extracted. Breakage of the CNT tip is attributed to separation of the individual CNTs within the tip due to the high electrical field. Vacuum annealing was found to improve the inter-nanotube bonding within the tip.

To record the emission pattern from the CNT tip the metal anode used in the above measurements was replaced with a phosphor-coated ITO (indium tin oxide) glass. The image formed on the phosphor screen by the emitted electrons was recorded by a CCD camera placed outside the vacuum chamber. Figure 4 shows the emission images obtained from a MWNT tip. A single emission spot was observed in all operating voltages, consistent with the SEM results, which showed that there is only one close-packed CNT tip anchored on each tungsten wire. At 1400 V the diameter of the bright spot on the phosphor screen is about 200 µm, giving a beam divergence angle of 50°. The large spread angle results from the
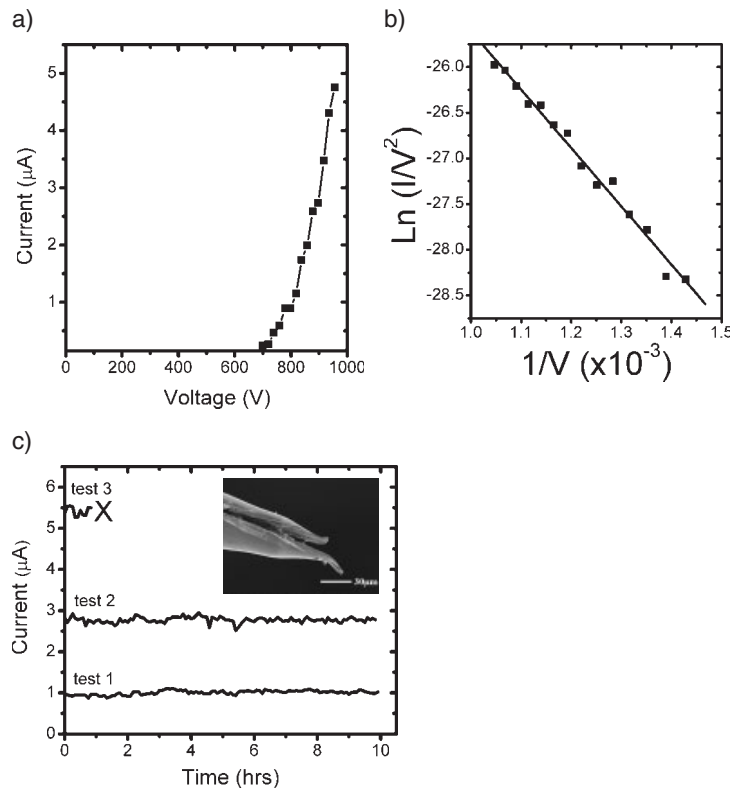
Figure 3. Electron-field-emission properties of a SWNT tip measured using point-plane geometry at 10^{-7} torr base pressure. The emission current–voltage characteristics (a) exhibited the classic Fowler–Nordheim type behavior with a linear relation between $\ln(I/V^2)$ and $1/V$ (b). Current stability was measured sequentially at 1 μA, 2.8 μA, and 5.5 μA when the applied voltage was fixed at 800 V, 1000 V, and 1200 V, respectively (c). A ballast resistor was put in series with the cathode. The cathode–anode distance was estimated to be ~200 μm. The inset is the SEM image of the W tip measured after failure showing fracture of the W and disappearance of the CNT tip.

electrical field distribution in the point–plane geometry rather than the intrinsic divergence angle of the field-emitted electrons from the nanotubes.

In summary, carbon nanotube tips with controllable length, diameter, and orientation have been fabricated by the dielectrophoresis process. This has not been achieved by other techniques. The tips with van der Waals' bonded nanotubes are mechanically rigid and retain their rigid rod-like morphology even when the length exceeds ~30 μm.[27] Due to the interfacial morphology they adhere strongly to the metal supports, which ensure stability under high electrical field and minimizes mechanical vibration. The CNTs are capable of delivering high and stable electron-field-emission currents that exceed 10^5 A cm^{-2} in density. Compared to the other techniques reported so far for making CNT tips, the present dielectrophoresis method is efficient, controllable, and reproducible. Parallel fabrication of multiple tips using the same CNT source at the same time has already been demonstrated. The emitters thus fabricated can potentially be used as the field-emission electron sources for precision vacuum electronic instruments such as electron microscopes.
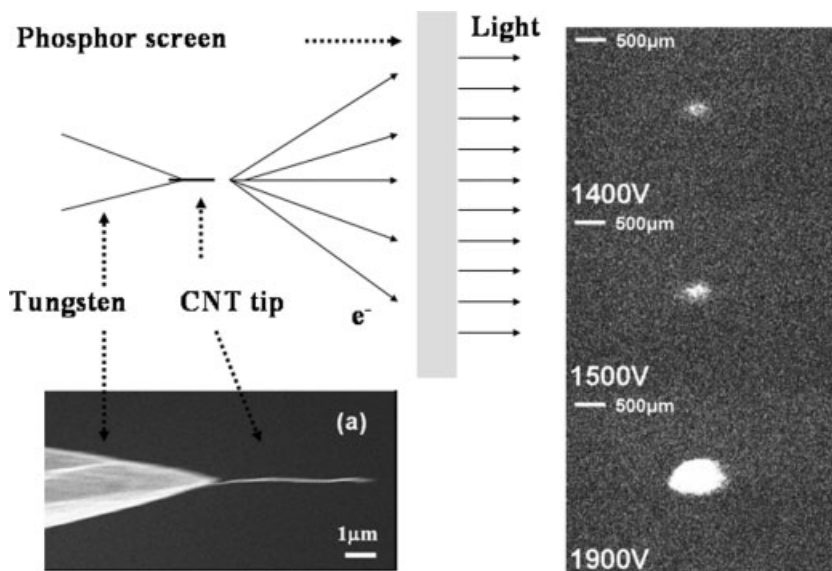
Figure 4. The emission images from a MWNT tip were recorded at different applied voltages. A single emission spot was observed in all operating voltages. The large divergence angle (50° at 1400 V) is due to the electrical field distribution in the point-plane geometry rather than the intrinsic divergence angle of the field-emitted electrons from the nanotubes.

[1] Y. Saito, S. Uemura, K. Hamaguchi, *Jpn. J. Appl. Phys., Part 2* **1998**, *37*, 346.

[2] N. S. Lee, D. S. Chung, I. T. Han, J. H. Kang, Y. S. Choi, H. Y. Kim, S. H. Park, Y. W. Jin, W. K. Yi, M. J. Yun, J. E. Jung, C. J Lee, J. H. You, S. H. Jo, C. G. Lee, J. M. Kim, *Diamond Rel. Mater.* **2001**, *10*, 265.

[3] G. Z. Yue, Q. Qiu, B. Gao, Y. Cheng, J. Zhang, H. Shimoda, S. Chang, J. P. Lu, O. Zhou, *Appl. Phys. Lett.* **2002**, *81*, 355.

[4] N. de Jonge, Y. Lamy, K. Schoots, T. H. Oosterkamp, *Nature* **2002**, *420*, 393.

[5] W. A. de Heer, A. Chatelain, D. Ugarte, *Science* **1995**, *270*, 1179.

[6] P. G. Collins, A. Zettl, *Appl. Phys. Lett.* **1996**, *69*, 1969.

[7] Y. Wei, C. G. Xie, K. A. Dean, B. F. Coll, *Appl. Phys. Lett.* **2001**, *79*, 4527.

[8] W. Zhu, C. Bower, O. Zhou, G. Kochanski, S. #Jin, *Appl. Phys. Lett.* **1999**, *75*, 873.

[9] K. A. Dean, B. R. Chalamala, *J. Appl. Phys.* **1999**, *85*, 3832.

[10] J. H. Hafner, C. L. Cheung, C. M. Lieber, *Nature* **1999**, *398*, 761.

[11] J. G. Wen, Z. P. Huang, D. Z. Wang, J. H. Chen, S. X. Yang, Z. F. Ren, J. H. Wang, L. E.

Calvet, J. Chen, J. F Klemic, M. A. Reed, *J. Mater. Res.* **2001**, *16*, 3246.

[12] C. L. Cheung, J. H. Hafner, T. W. Odom, K. Kim, C. M. Lieber, *Appl. Phys. Lett.* **2000**, *76*, 3136.

[13] S. S. Wong, A. T. Woolley, T. W. Odom, J.-L. Huang, P. Kim, D. Vezenov, C. M. Lieber, *Appl. Phys. Lett.* **1998**, *73*, 3465.

[14] H. Nishijima, S. Kamo, S. Akita, Y. Nakayama, K. I. Hohmura, S. H. Yoshimura, K. Takeyasu, *Appl. Phys. Lett.* **1999**, *74*, 4061.

[15] S. Akita, H. Nishijima, Y. Nakayama, F. Tokumasu, K. Takeyasu, *J. Phys. D* **1999**, *32*, 1044.

[16] M. Milas, R. Foschia, A. Kulik, R. Gaál, E. Ljubovic, L. Forró, *AIP Conf. Proc.* **2002**, *633*, 614.

[17] T. B. Jones, *Electromechanics of Particles*, Cambridge University Press, Cambridge, UK **1995**.

[18] O. D. Velev, E. W. Kaler, *Langmuir* **1999**, *15*, 3693.

[19] W. B. Choi, J. J. Cuomo, V. V. Zhirnov, A. F. Myers, J. J. Hren, *Appl. Phys. Lett.* **1996**, *68*, 720.

[20] J. Tang, B. Gao, H. Geng, O. D. Velev, L.-C. Qin, O. Zhou, *Adv. Mater.* **2003**, *15*, 1352.

[21] O. Zhou, H. Shimoda, B. Gao, S. J. Oh, L. Fleming, G. Z. Yue, *Acc. Chem. Res.* **2002**, *35*, 1045.

[22] J. Liu, A. G. Rinzler, H. Dai, J. H. Hafner, R. K. Bradley, P. J. Boul, A. Lu, T. Iverson, K. Shelimov, C. B. Huffman, F. Rodriguez-Macias, Y. Shon, T. R. Lee, D. T. Colbert, R. E. Smalley, *Science* **1998**, *280*, 1253.

[23] S. J. Oh, Y. Cheng, J. Zhang, H. Shimoda, O. Zhou, *Appl. Phys. Lett.* **2003**, *82*, 2521.

[24] S. Niyogi, M. A. Hamon, H. Hu, B. Zhao, P. Bhowmik, R. Sen, M. E. Itkis, R. C. Haddon, *Acc. Chem. Res.* **2002**, *35*, 1105.

[25] C. Bower, O. Zhou, W. Zhu, D. J. Werder, S. H. Jin, *Appl. Phys. Lett.* **2000**, *77*, 2767.

[26] K. A. Dean, B. R. Chalamala, *Appl. Phys. Lett.* **1999**, *75*, 3017.

[27] F. Tsui, unpublished.

Cerium Compound Nanowires and Nanorings Templated by Mixed Organic Molecules**

By *Mitsunori Yada,* Seiji Sakai, Toshio Torikai, Takanori Watari, Sachiko Furuta,* and *Hiroaki Katsuki*

One-dimensional structures such as nanowires, nanofibers, and nanoribbons with high aspect ratios have attracted much attention lately due to their high potential for applications in fabricating electronic devices, sensors, etc. These structures are expected to have their unusual characteristics amplified

[*] Dr. M. Yada, S. Sakai, T. Torikai, Dr. T. Watari
Department of Chemistry and Applied Chemistry
Faculty of Science and Engineering, Saga University
1 Honjo, Saga 840-8502 (Japan)
E-mail: yada@cc.saga-u.ac.jp
Dr. S. Furuta, Dr. H. Katsuki
Saga Ceramics Research Laboratory
3037-7, Arita, Saga 844-0024 (Japan)

through quantum size effects, and marked shape-specific effects.[1–3] To obtain one-dimensional materials, organic molecules are often used as a medium or template. The use of sodium bis(2-ethylhexyl)sulfosuccinate (NaAOT) represents an especially powerful tool to synthesize nanowires of materials such as $CaSO_4$,[4] $BaSO_4$,[5] Cu,[6] $BaCrO_4$,[7] $BaWO_4$,[8] and CdS.[9] Less-ordered hexagonal mesostructured SnO_2, templated by NaAOT has also been reported.[10]

Ceria (CeO_2) and ceria-based materials have been extensively used as solid electrolytes in solid oxide fuel cells; as automotive catalysts, utilizing their oxygen storage capacity; as absorbents for fluoride ion or arsenic-based compounds; and as substances to filter out ultraviolet rays. Ceria and ceria-based compounds obtained in nanostructured forms are thus expected to be promising as materials that show interesting properties through shape-specific and/or quantum size effects. Nanostructured ceria, synthesized using organic molecules, has been previously reported in the literature. Masui et al. reported the synthesis of monodisperse ceria nanoparticles with diameters of 2.6 nm in reverse micelles composed of AOT (bis(2-ethylhexyl)sulfosuccinate) anions.[11] Less-ordered mesoporous ceria was synthesized using alkyltrimethylammonium bromide as a template.[12] Ordered mesoporous ceria templated by hexadecylamine has also been reported.[13] Macroporous ceria was obtained by a nanotectonic approach based on the template-directed assembly of organically functionalized ceria crystalline particles by poly(γ-benzyl-L-glutamate).[14]

In this paper, we report for the first time the synthesis of cerium compound nanowires and nanorings templated by AOT anions and alkyl alcohols. We also demonstrate nanostructural control of the cerium compound nanostructures by the carbon number of the incorporated alkyl alcohol.

Figure 1a shows the transmission electron microscopy (TEM) image of a solid synthesized in the presence of NaAOT after a reaction time of 5 h. Nanowires were obtained with widths of several tens of nanometers and lengths of the order of micrometers. The sulfur to cerium, or AOT to cerium molar ratio, determined by energy dispersive X-ray (EDX) analysis was 0.37, indicating that AOT molecules were incorporated in the solid. Figure 1b is an enlarged image of the nanowire and shows stripes, suggesting the formation of a layered structure composed of a cationic cerium-based inorganic sheet with a thickness of 2.0 nm, and an anionic AOT bilayer with a thickness of 1.0 nm, as shown in the schematic representation of Figure 2. When the synthesis was performed in the presence of both butyl alcohol and NaAOT, instead of only NaAOT, similar but more divided nanowires were observable, as shown in Figures 1c–e. These nanowires also indicated a relatively ordered, layered structure composed of an inorganic sheet with a thickness of 2.1 nm and an organic molecular bilayer with a thickness of 1.4 nm, as determined from the higher magnification image Figure 1c. Figures 1d,e show a disordered layered structure observed in the same sample. The variations in the widths of the stripes strongly suggest that the nanowire substance has either an ordered or a disordered,